Optimization of Foraging Multi-Agent System Front: A Flux-Based Curve Evolution Method

Musad Haque, Amir Rahmani, Magnus Egerstedt, and Anthony Yezzi

***Abstract*— Numerous social foragers form a foraging front that sweeps through the aggregation of prey. Based on this strategy, and using variational arguments, we develop an algorithm to provide a group-level specification of the shape of the sweeping front for a foraging multi-robot system. The presented flux-based algorithm has the desired property of generating more regular shapes than previously introduced algorithms.**

I. INTRODUCTION

As a foraging technique, predators often directly charge through an aggregation of prey. Examples of such predators include African lions, *Panthera leo*, Bottlenose dolphins, *Tursiops truncatus*, and Cheetahs, *Acinonyx jubatus* [1], [2], [3]. Although groups of Cheetahs often hunt together, there is no coordination between members of the group: individuals "sprint into a herd of prey" and behave selfishly [4]. On the other end of this cooperation spectrum, African lions and Bottlenose dolphins exhibit a high degree of coordination while foraging prey [1], [2]. These biological systems charge though the aggregation of prey, in unison, by forming a foraging front. The shape of the foraging front differs for these systems - lions form a shape that is described as a "catcher's mitt" in [1], while dolphins move line abreast [2]. In this paper, we draw inspiration from the strategy used by these social animals and optimize the shape of predator fronts for a foraging multi-agent system.

Foraging has received substantial attention in the multi-robot community (for a representative sample, see [5], [6], [7], [8], [9]). While previous works have focused on the search and retrieval aspects of stationary objects or cooperative agents, we focus on the geometric shape of the foraging front. The predator front is modeled as a curve that sweeps through the aggregation of prey. As a result, we are assuming a continuum of predators instead of the common agent-based model of foragers seen in [9]. Starting with an initial estimate of the shape of the optimal curve, we calculate the the total energy intake (total amount of prey consumed) during a sweep through the collection of prey. The shape of the curve is then deformed according to a curve flow algorithm so that the energy intake of the curve is maximized.

The curve flow algorithm is based on curve evolution techniques. These techniques are widely used for image segmentation purposes (for a representative sample, see [10], [11], [12]), where active contours evolve a curve under an optimality condition to detect objects. In this work, an arc length parametrized curve is evolved according to a gradient ascent based deformation algorithm. Potential applications for this work are recovery tasks, such as the clean up of chemical spills. We propose to utilize a multi-robot system for an efficient clean up task of spilled chemicals, as shown in Fig. 1, where a group of robots coordinate to drive a flexible suction boom towards the spill site. For an efficient recovery, the shape of the boom can be optimized using the curve flow algorithm developed in this work.

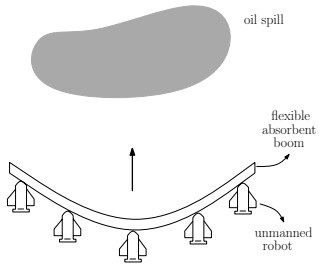

Fig. 1. A group of unmanned vehicles are driving a flexible, absorbent boom towards an oil spill. Optimizing the shape of the boom, to remove the largest amount of oil, is a possible application of the proposed curve flow algorithm.

The remainder of the paper is organized as follows: In Section II, we introduce the curve-based model of the foraging front. In Section III, we discuss the nature of the curve flow algorithm presented in [14], and in Section IV, we develop a curve flow algorithm that addresses some of the deficiencies of the algorithm derived in [14]. Simulations are shown in Section V, and discussion are provided in Section VI. Finally, conclusions are presented in Section VII.

II. PREDATOR FRONT MODEL

Let the predator front be given by the curve, $C(s,t,\tau)$, where s is the arclength parameter, t denotes time, and $\tau \in \mathbb{R}$ parameterizes a family of time-varying curves. We denote the total length of the curve by $L(\tau)$; thus, $s \in [0, L(\tau)]$. The main idea of the algorithm is to start with an initial estimate of the shape of the curve, $C(s,t,0)$, and let it sweep through the aggregation of prey from $t = 0$ to $t = t_f$. The energy intake is computed and then the shape of the curve is deformed (with respect to τ) such that the energy intake is increased during the next sweep. We repeat these steps until the best curve shape is found. Hence, we determine the optimum shape of the front by evolving the curve using

This work was partially supported by the Office of Naval Research through the MURI-HUNT.

M. Haque, A. Rahmani, M. Egerstedt, and A. Yezzi are with School of Electrical and Computer Engineering, Georgia Institute of Technology, Atlanta, GA 30332, USA email: musad.haque@gatech.edu, {arahmani, magnus, ayezzi}@ece.gatech.edu

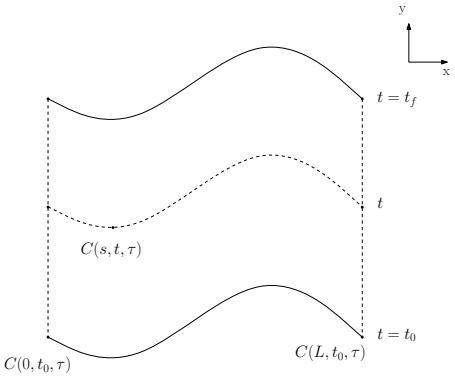

Fig. 2. A curve front sweeps in the positive y direction with unit speed while maintaining its shape.

.

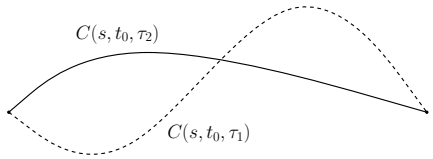

Fig. 3. Curves evolving under the proposed algorithm share the same endpoints at $t = t_0$.

gradient ascent and moving in a direction that increases the energy intake.

As such, the shape of the predator front remains fixed during a sweep through the aggregation of prey, as shown in Fig. 2. Moreover, without loss of generality, we assume that the front sweeps the area with unit speed and in the positive y direction. Also, we assume that all curve shapes have identical endpoints, i.e. the endpoints of the curve stay the same regardless of the deformation in the shape of the curve, as shown in Fig. 3.

We have addressed the problem of characterizing the optimal shape of the foraging front in [13] and [14]. In [13], this effort was restricted to the simulation of quadratic curves under various predator-prey interactions. In [14], a curve flow algorithm was developed based on curve evolution techniques, but the algorithm - due to the formulation of the energy function - has a major drawback. In the next sections, we discuss the deficiency of the algorithm presented in [14] and address this issue by reformulating the energy function of the predator front.

III. Length-Constrained Evolution

In [14], the energy-intake during a sweep of the curve, i.e. the amount of prey being consumed during a charge, is given by

$$E'(\tau) = \int_0^{t_f} \int_0^{L(\tau)} u(C(s,t,\tau),t)\ ds\ dt, \qquad (1)$$

where $u : \mathbb{R}^2 \times \mathbb{R} \to \mathbb{R}$ describes prey density at position (x, y) at time t. Thus, $u(C(s,t,\tau),t)$ denotes the amount of prey consumed by the curve at the position $C(s,t,\tau)$ at time t. Based on this formulation of the energy-intake, the following curve evolution is proposed:

$$C_\tau := \Big[\overrightarrow{N}^T \int_0^{t_f} \nabla u^T\ dt - \kappa \int_0^{t_f} u\ dt\Big]\overrightarrow{N}, \qquad (2)$$

where, $\nabla u(C(p,t,\tau),t)$ is the $2D$ spatial gradient of u, $\kappa(s,\tau)$ is the curvature, and $\overrightarrow{N}(s,\tau)$ is the unit normal. (For conciseness, we let f_x represent the partial derivative $\partial f/\partial x$ of a function $f(x,y)$ and denote the second-order partial derivative $\partial f/\partial x \partial y$ by f_{xy}.)

Note that this evolution stems from a fairly intuitive formulation of the energy function, E: the energy intake of the front is the sum of the prey it sweeps over time. However, this formulation places no restriction on the length of the curve. Moreover, since $\kappa \int_0^{t_f} u\ dt\overrightarrow{N} > 0$, it represents a backward diffusion term in (2), and will generate infinitely long curves to increase the energy.

An alternative energy function is provided in [14] that also penalizes the length of the curve. This energy-intake is formulated as follows:

$$E''(\tau) = E'(\tau) - \rho L(\tau), \qquad (3)$$

where $E'(\tau)$ is the energy function given by (1), $L(\tau)$ is the length of the curve, and ρ is some positive constant used to regulate the length of the curve. The result is a *length-constrained curve evolution* given by

$$C_\tau := \Big[\overrightarrow{N}^T \int_0^{t_f} \nabla u\ dt - \kappa\left(\int_0^{t_f} u\ dt - \rho\right)\Big]\overrightarrow{N}, \qquad (4)$$

that prevents the formation of infinitely long curves, but the tendency of the curves remain the same: add more length to maximize energy. This behavior of the curve can be seen in Fig. 4, where the prey density evolves according to a pure diffusion process. More specifically, the movement of prey is described by the following equation:

$$\frac{\partial u(x,y,t)}{\partial t} = v_0\left(\frac{\partial^2 u(x,y,t)}{\partial x^2} + \frac{\partial^2 u(x,y,t)}{\partial y^2}\right), \qquad (5)$$

where $v_0 \in \mathbb{R}_+$ is the thermal diffusivity. The prey diffuses from its initial density, $u(x,y,0)$, at a "speed" of v_0, regardless of the location of the predator front. Due to this choice of design for the prey dynamics, during a sweep of the curve, a greater concentration of prey remains at the location of the initial density. Thus, the overall tendency of the resulting curve is to place more length in the area where there is a high initial density of prey. As such, after every iteration of τ, the curve adds more length in the locations with higher prey density. The curve eventually takes a sawtooth-like shape.

In the next section, we introduce an evolution that has the desired property of generating more regular shapes than the sawtooth-like shapes generated by (4).

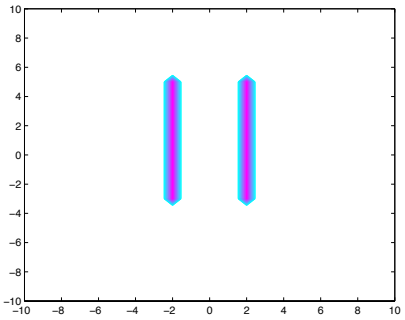

(a) Initial distribution of prey.

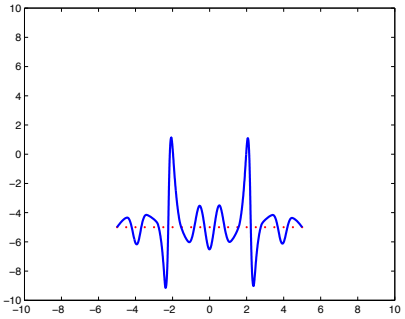

(b) The optimized curve.

Fig. 4. A curve is deformed according to (2). Since there is no restriction on the length of the curve, after every iteration of τ, the curve adds more length in the locations with higher prey density. The prey movement is given by the diffusion process of (5). The dotted line in (b) shows the initial estimate of the shape of the curve.

IV. FLUX-BASED EVOLUTION

For the energy functions used in [14] (see previous section) and the resulting curve evolutions (2) and (4), we essentially produce shapes that maximize the overall energy intake if there is *instantaneous replacement* of the prey. For example, consider the scenario where the agents configure themselves in a line, parallel to the direction of the sweep. According to (1), we would still maximize $u(C(s,t,\tau),t)$ along this curve during the sweep. Thus, when an agents passes through a location, it does not affect the consumption of all the agents that follow it. In essence, there is *no conservation of prey*. In this work, we design a curve evolution that maintains the conservation of prey. More specifically, we consider the total flux of the vector $u(C(s,t,\tau),t)C_t(s)$ through the curve. Here, the flux, which is inherently a differential in mass, corresponds to consumed prey.

Since the curve front sweeps in the positive y direction with unit speed, the flux lines of $u(C(s,t,\tau),t)C_t(s)$ points in the positive y direction. The new formulation for the energy-intake during a sweep of the curve is given by

$$E(\tau) = \int_0^{t_f} \int_0^{L(\tau)} F \cdot \overrightarrow{N}\ ds\ dt, \tag{6}$$

where, $F = u(C(s,t,\tau),t)C_t(s)$.

To find an expression for the curve evolution C_τ, we first take the derivative of the energy function with respect to τ. With this expression of C_τ, the shape of the curve is updated so that the gradient of $E(\tau)$ with respect to τ is increased. To compute this derivative, we introduce a parameter $p \in [0,1]$ to replace the s parameterization of the curve with a parameterization that is not τ dependent. (For this substitution, we follow the method outlined in [14].) From the definition of arc length,

$$L(\tau) \quad = \quad \int_0^{L(\tau)} ds = \int_0^1 \|C_p(p,\tau)\|\ dp, \tag{7}$$

from which it follows that

$$ds = \|C_p(p,\tau)\|\ dp. \tag{8}$$

As a result, $dE(\tau)/d\tau =$

$$\int_0^{t_f} \int_0^1 F_\tau \cdot \overrightarrow{N}\|C_p\| + F \cdot \overrightarrow{N}_\tau \|C_p\| + F \cdot \overrightarrow{N}\|C_p\|_\tau\ dp\ dt. \tag{9}$$

Note that $F_\tau = J_F C_\tau$, where J_F is the Jacobian of F. Also, we have that

$$\|C_p(p,\tau)\|_\tau^2 = 2\|C_p(p,\tau)\|\|C_p(p,\tau)\|_\tau, \tag{10}$$

and

$$(C_p^T C_p)_\tau = 2C_{p\tau}^T C_p, \tag{11}$$

where the superscript T denotes transpose. As a result,

$$\|C_p\|_\tau = C_{p\tau}^T \frac{C_p}{\|C_p\|} = C_{\tau p} \cdot \overrightarrow{T}(p,\tau), \tag{12}$$

where, note that the partial derivatives of C can be exchanged and we introduce the unit tangent of the curve,

$$\overrightarrow{T}(p,\tau) = \frac{C_p}{\|C_p\|}. \tag{13}$$

Thus, $dE(\tau)/d\tau =$

$$\int_0^{t_f} \int_0^1 J_F C_\tau \cdot \overrightarrow{N}\|C_p\| + F \cdot \overrightarrow{N}_\tau \|C_p\| + F \cdot \overrightarrow{N} C_{\tau p} \cdot \overrightarrow{T}\ dp\ dt. \tag{14}$$

From the definition of an outward normal, $\overrightarrow{N} = R\overrightarrow{T}$, where R is the $\pi/2$ clockwise rotation matrix,

$$\begin{aligned} \overrightarrow{N}_\tau &= (R\overrightarrow{T})_\tau \\ &= \frac{1}{\|C_p\|} R(C_{\tau p} - \overrightarrow{T} C_{\tau p} \cdot \overrightarrow{T}) \\ &= \frac{1}{\|C_p\|} R\overrightarrow{N} C_{\tau p} \cdot \overrightarrow{N} \\ &= \frac{-C_{\tau p} \cdot \overrightarrow{N}}{\|C_p\|} \overrightarrow{T}. \end{aligned} \tag{15}$$

Hence, we can now write $dE(\tau)/d\tau =$

$$\int_0^{t_f} \int_0^{L(\tau)} J_F C_\tau \cdot \overrightarrow{N} - F \cdot (C_{\tau s} \cdot \overrightarrow{N}\overrightarrow{T}) + F \cdot \overrightarrow{N} C_{\tau s} \cdot \overrightarrow{T}\ ds\ dt, \tag{16}$$

when we switch back to the s parameterization. Furthermore, using integration by parts and by noting that $\overrightarrow{N}_s = R\overrightarrow{T}_s = \kappa\overrightarrow{T}$, $F_s = J_F C_s = J_F\overrightarrow{T}$, and $J_F C_\tau \cdot \overrightarrow{N} \in \mathbb{R}$, we have $dE(\tau)/d\tau =$

$$\begin{aligned}
& \int_0^{t_f}\int_0^{L(\tau)} C_\tau \cdot J_F^T\overrightarrow{N} + (J_F\overrightarrow{T})\cdot\overrightarrow{T}C_\tau\cdot\overrightarrow{N} \\
- \;& (J_F\overrightarrow{T})\cdot\overrightarrow{N}C_\tau\cdot\overrightarrow{T}\; ds\; dt \\
= \;& \int_0^{t_f}\int_0^{L(\tau)} C_\tau\cdot\left[\overrightarrow{N}^T J_F\overrightarrow{N} + \overrightarrow{T}^T J_F\overrightarrow{T})\right]\overrightarrow{N}\; ds\; dt \\
= \;& \int_0^{t_f}\int_0^{L(\tau)} C_\tau\cdot\left[tr(J_F)\overrightarrow{N}\right]\; ds\; dt \\
= \;& \int_0^{t_f}\int_0^{L(\tau)} C_\tau\cdot(\nabla\cdot F\overrightarrow{N})\; ds\; dt, \qquad (17)
\end{aligned}$$

where, $tr(\cdot)$ represents the trace of a matrix and $\nabla\cdot F$ denotes the divergence of the vector field F. With this expression for $dE(\tau)/d\tau$, we choose the following curve evolution:

$$C_\tau = \int_0^{L(\tau)}\int_0^{t_f} \nabla\cdot F\; dt\; \overrightarrow{N}\; ds. \qquad (18)$$

For this *flux-based curve evolution*, $dE(\tau)/d\tau$ is non-negative, and the update rule for the curve becomes

$$C(s,0,\tau_{next}) = C(s,0,\tau) + (\tau_{next}-\tau)C_\tau(s,\tau), \qquad (19)$$

except at the endpoints, where the curve shape does not change.

V. SIMULATIONS

The foraging area is represented as a $2D$ mesh, where $x_{min} = -10$, $x_{max} = 10$, $y_{min} = -10$, $y_{max} = 10$, and the mesh spacing is $\Delta x = \Delta y = 0.5$. For each τ, the resulting curve is swept through the prey density from $t_i = 0$ to $t_f = 20$, with a time step of $\Delta t = 0.005$. We use 21 data points to characterize a curve and the initial estimate of the shape of the curve (at $\tau = 0$) is a straight line.

In Fig. 5, the curve is updated according to the flux-based evolution of (18). Three different initial configurations of prey are used, and the prey evolves according to the diffusion process given by (5). Further, for each configuration, the resulting curve is shown for different speeds of prey diffusion, v_0.

VI. DISCUSSIONS

Based on the simulation results, we show how the location of the peaks, and their quality, depend on factors like the initial configuration and diffusion speed of the prey.

A. Location of Peaks

For the flux-based evolution, we notice that the locations of the peaks depend on the initial configuration of the prey. This results holds for the length-constrained evolution as well, as already shown in [14]. This characteristic of the optimal curve can be attributed to our design of the aggregation of prey. With a pure diffusion equation representing the movement of prey, there is essentially no predator-prey interaction [15] and the highest concentration of prey remains in the positions where prey is initially located.

B. Quality of Peaks

As the diffusion speed increases, we notice that the flux-based evolutions tend to generate wider peaks and as a result, the curves tend to be "flatter."

As mentioned in Section IV, the flux-based evolutions have a nice property in that it generates curves that have a more regular shape than the length-constrained curves. Another property that was mentioned in that section was the fact that the nature of the energy function (and the resulting evolution) conserved mass. This property tries to prevent agents on the curve from arranging themselves one behind the other. In Figs. 5(d)-(f), it may appear that this property is violated; however, since the prey is barely diffusing ($v_0 = 0.001$), there is no incentive for the agents to space out. As a result, they align one behind the other like the length-constrained curve.

VII. CONCLUSION

We optimize the shape of a foraging front that sweeps through an aggregation of prey. Potential applications of this work include the design of a suction boom for surface chemical skimming using a multi-robot system. The predator front is modeled as a curve and using curve evolution techniques, a curve flow algorithm is developed that maximizes the energy-intake of the curve. The energy function for the curve is formulated in a manner that conserves mass. Based on this formulation, the curve flow algorithm maximizes the flux along the curve, which is in turn given by a prey density function. As such, the algorithm does not depend on the movement laws governing the collection of prey, it only requires knowledge of the amount of prey located at a position for any given time. Simulations show that the certain characteristics of the curve, e.g. location of peaks, depend on factors like the initial configuration of prey.

REFERENCES

[1] R.D. Estes, *Behavior Guide to African Mammals*, University of California Press, Berkeley, CA; 1991.

[2] K. Pryor and K. Norris, *Dolphin Societies*, University of California Press, Berkeley, CA; 1998.

[3] T.M. Caro, *Cheetahs of the Serengeti Plains: group living in an asocial species*, The University of Chicago Press, Chicago, IL; 1994.

[4] P.E. Stander, Notes on foraging habits of cheetah, *S.-Afr. Tydskr. Natuurnav*, vol. 20, no. 4, 1990.

[5] D.A. Shell and M.J. Matarić, "On foraging strategies for large-scale multi-robot systems", *Intl. Conf. on Intelligent Robots and Systems*, Beijing, China, 2006, pp. 2717–2723.

[6] T. Balch, "The impact of diversity on performance in multi-robot foraging", *Proc. Third Conf. on Autonomous Agents*, Seattle, WA, 1999, pp. 92–99.

[7] T.H. Labella, M. Dorigo, and J. Deneubourg, "Self-organised task allocation in a group of robots", *Distributed Autonomous Robotic Systems*, 2004.

[8] N. Lemmens, S. Jong, K. Tuyls, and A. Nowé, "Bee Behaviour in Multi-agent Systems", *Adaptive Agents and Multi-Agent Systems III. Adaptation and Multi-Agent Learning*, 2008, pp. 145–156.

[9] G. Ferrari-Trecate, M. Egerstedt, A. Buffa and M. Ji, Laplacian Sheep: A Hybrid, Stop-Go Policy for Leader-Based Containment Control, *Hybrid Systems: Computation and Control*, Springer-Verlag, 2006, pp. 212–226.

[10] Y. Shi and W. Karl, A fast level set method without solving PDEs, *Int. Conf. on Acoustics, Speech, and Signal Processing*, 2005, pp. 97–100.

[11] T. Chan and L. Vese, "Active contours without edges," *IEEE Transactions on Image Processing*, vol. 10, no. 2, 2001, pp. 266–277.

[12] S. Lankton, D. Nain, A. Yezzi, and A. Tannenbaum, "Hybrid Geodesic Region-Based Curve Evolutions for Image Segmentation", *SPIE Medical Imaging*, San Diego, CA, 2007.

[13] M. Haque, A. Rahmani, and M. Egerstedt, "Geometric Foraging Strategies in Multi-Agent Systems Based on Biological Models," *Conference on Decision and Control*, Atlanta, USA, Dec 2010.

[14] M.A. Haque, A.R. Rahmani, M. Egerstedt, and A. Yezzi, "Biologically Motivated Shape Optimization of Foraging Fronts", *American Control Conference*, San Francisco, USA, 2011.

[15] J.D. Murray, *Mathematical Biology I: An Introduction*, Springer, New York, NY; 2002.

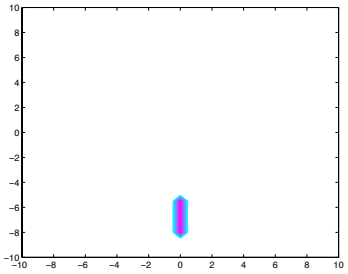

(a) Initial configuration of prey.

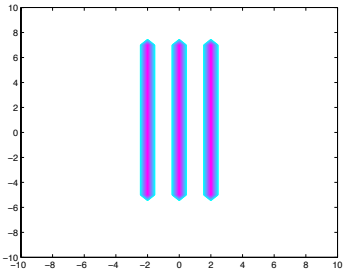

(b) Initial configuration of prey.

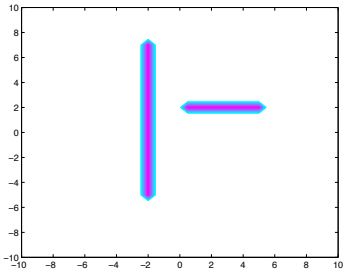

(c) Initial configuration of prey.

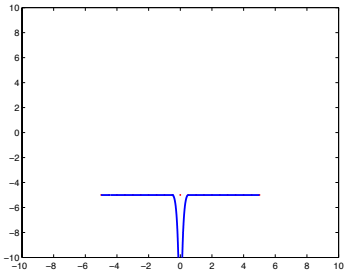

(d) $v_0 = 0.001$

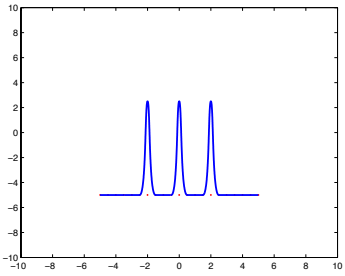

(e) $v_0 = 0.001$

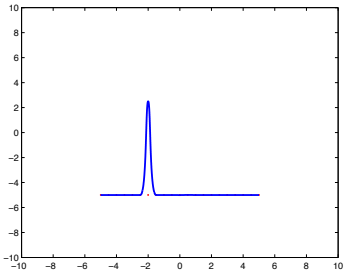

(f) $v_0 = 0.001$

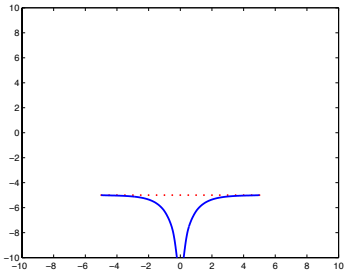

(g) $v_0 = 0.5$

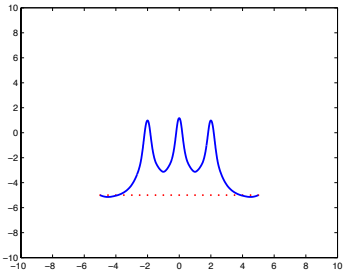

(h) $v_0 = 0.5$

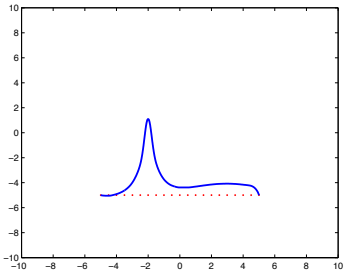

(i) $v_0 = 0.5$

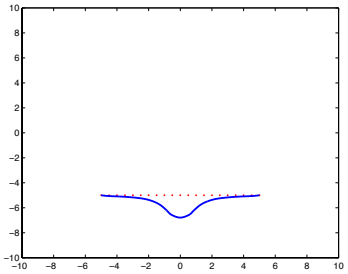

(j) $v_0 = 1.0$

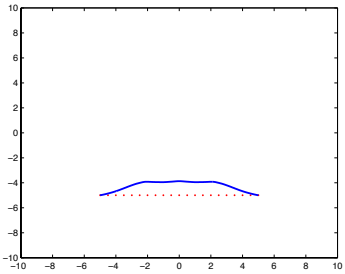

(k) $v_0 = 1.0$

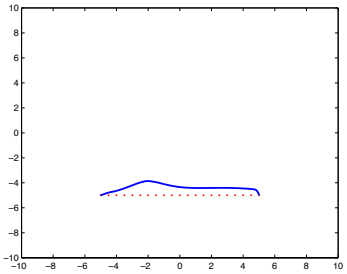

(l) $v_0 = 1.0$

Fig. 5. The top row shows three different initial configurations of the prey density. Underneath each configuration are three figures showing the optimized curve according to the flux-based evolution for different diffusion speeds. The dotted lines represent the initial estimate of the shape of the curve. Note that the peaks of the curves tend to widen when the speed of diffusion of the prey increases.